

DEVELOPMENT OF THE TECHNOLOGY OF PRODUCING A BIOCOMPATIBLE ALLOY BASED ON ZIRCONIUM–TITANIUM–NIOBIUM SYSTEM FOR MEDICAL IMPLANTS

O.V. Ovchynnykov¹, V.O. Berezos², V.S. Yefanov³, D.S. Akhonin², D.I. Mozulenko⁴

¹JSC “Institute of Titanium”

180 Sobornyy Prosp., 69035, Zaporizhzhia, Ukraine

²E.O. Paton Electric Welding Institute of the NASU

11 Kazymyr Malevych Str., 03150, Kyiv, Ukraine

³Ukrainian State University of Science and Technology

2 Lazaryan Str., 49010, Dnipro, Ukraine

⁴National University “Zaporizhzhia Polytechnic”

64 Zhukovski Str., 69063, Zaporizhzhia, Ukraine

ABSTRACT

The paper gives an overview of development and application of biocompatible alloys based on zirconium, titanium and niobium, featuring a low modulus of elasticity. The technology of producing a biocompatible 60Zr–20Ti–20Nb alloy and semi-finished products from it in the form of rods and powders for additive manufacturing was developed, and their structure and mechanical properties were studied. The potential for application of the developed biocompatible 60Zr–20Ti–20Nb alloy for manufacturing medical implants is shown.

KEYWORDS: zirconium, titanium, niobium, biocompatible alloys, electron beam melting, technological modes, chemical composition, structure, modulus of elasticity, mechanical properties

INTRODUCTION

Over the recent decades considerable attention was given to development and investigation of new materials for the medical industry, particularly in the field of implant creation. Modern implants require application of materials which are characterized not only by high biochemical compatibility and strength, but also special functional properties, such as shape memory, low modulus of elasticity, etc. [1–3]. One of the dominating criteria of application of metals for medical purposes is the criterion of survival of implants made from these materials in the human body.

At first a lot of attention was given to commercial titanium alloys of Ti–6Al–4V, Ti–6Al–7Nb type [4, 5], but the negative aspects appeared rather quickly. Titanium-based alloys have higher rigidity (Young’s modulus, 110–120 GPa), which is three times higher than the value of bone rigidity (20–30 GPa) [6]. This difference leads to so-called voltage screening effect, causing bone resorption around the implant and leading to disintegration processes, i.e. creating a high degree of biomechanical incompatibility. Moreover, these alloys release toxic ions of vanadium and aluminium into the human body, leading to long-term processes of restoration of vital functions of the body.

In a separate set of polyfunctional biomedical materials a particularly important place is taken up by low-modulus titanium alloys, differing by a complex of extremely important characteristics: high ductility and strength, corrosion resistance and biocompatibility, owing to its biomechanical properties [7].

At present the achievements in the field of development of metallic biomaterials are focused on new variants of titanium-zirconium alloy, which are free of toxic elements, and have much lower modulus of normal elasticity (40–80 GPa). The low-modulus alloys based on zirconium-titanium compositions, while corresponding to biocompatibility criterion, also provide the technological capabilities at their manufacture by currently available methods, and ensure good prospects in the area of application of both the traditional technologies of manufacturing serial implants, and advanced additive technologies for individual implants [8].

Investigations of the equilibrium constitutional diagram of Ti–Zr system point to the rationality of development of alloys for medical purposes with zirconium content of 35–50 at.%. Minimal temperatures of melting and polymorphous transformation correspond to this range. It should be noted that martensite transformation is characteristic for Ti–Zr alloys at cooling, so that additional alloying, for instance by niobium, is used. Such alloying not only ensures a lowering of polymorphous

Table 1. Composition of zirconium master alloy (main alloying elements), wt.% (not more than)

| Grade | N | O | C | Fe | S | Ni | Cl | Al | Ca | Mn | Ti | Cr |
|------------------|-------|------|-------|-------|-------|------|-------|-------|------|-------|-------|-------|
| Iodide zirconium | 0.005 | 0.05 | 0.008 | 0.03 | 0.008 | 0.02 | — | 0.005 | 0.02 | 0.001 | 0.005 | 0.02 |
| KTTs-110 | 0.006 | 0.14 | 0.020 | 0.030 | 0.010 | 0.01 | 0.003 | 0.005 | 0.01 | 0.001 | 0.007 | 0.005 |

Table 2. Composition of titanium sponge, wt.% (not more than)

| Grade | N | O | C | Fe | Si | Ni | Cl |
|--------|------|------|------|------|------|------|------|
| TG-90 | 0.02 | 0.04 | 0.02 | 0.05 | 0.01 | 0.04 | 0.08 |
| TG-120 | 0.02 | 0.06 | 0.03 | 0.11 | 0.02 | 0.04 | 0.08 |

transformation temperature, but it also allows fixing by hardening the state with minimal values of the modulus of elasticity. Here, a high ductility is preserved.

Wide-spread application of low-modulus Ti–Zr alloys is limited by the complexity and multistage nature of the technological process of producing wrought semi-finished products in the technological schemes of manufacturing the implants — 6 mm diameter rods and 50–60 mm diameter electrodes for spraying the powders used in additive processes. A separate problem is producing ingots of Ti–Zr alloys with homogeneous chemical and phase composition of the metal in the product volume to provide a uniform distribution of deformation efforts inside the next semi-finished products and end products. Titanium, zirconium and niobium are chemically active elements, requiring methods of melting in vacuum. An essential difference between the metals in the density and melting temperatures, as well as technological difficulties in charge preparation, limits the possibilities for application of a number of vacuum melting methods. In keeping with analysis of works [9–11], the most rational technique is the method of electron beam melting (EBM). However, there is a range of unsolved issues as to the technological modes of melting, number of remelting cycles and determination of element transition coefficients.

OBJECTIVE

of this investigation was to produce a low-modulus zirconium β -alloy and to manufacture and study the characteristics of billets for implants from this alloy, which ensures the required level of mechanical and special properties determined by the medical purpose.

The alloy forms with application of chemically active elements, which requires special production conditions. In particular, it is necessary to conduct the melting process under vacuum and apply special techniques for averaging the chemical composition, stabilization of temperature and concentration parameters of alloy ingot formation. The above conditions of formation of the alloy and ingots from it are provided by cold-hearth electron beam melting.

Thus, this study is a complex analysis of the properties and application of 60Zr–20Ti–20Nb alloy, emphasizing its significance and good prospects for medical industry, particularly in the context of improvement of the quality and safety of medical implants.

INVESTIGATION MATERIALS AND METHODS

In order to develop 60Zr–20Ti–20Nb alloy with predicted properties, two different charges of the following composition were used: charge 1 — zirconium iodide, niobium and titanium sponge (TG-120); charge 2 — zirconium KTTs-110, niobium and titanium sponge (TG-90).

In order to lower the cost of charge materials, zirconium of KTTs-110 grade was used instead of zirconium iodide in charge composition 2 to produce experimental Zr–Ti–Nb alloy. Despite the fact that KTTs-110 zirconium has a higher concentration of oxygen, titanium sponge TG-90 was used in charge 2 for equalizing the amount of oxygen in the final alloy. Element composition of the raw material is given in Tables 1–3, and the material used — in Figure 1.

Alloying element content in the ingots was determined by the method of inductively-coupled plasma. Methods of optical emission spectrometry (ICP-OES) were applied using ICP-spectrometer ICAP 6500 DUO.

Samples for metallographic studies were polished using an abrasive disc (240–400–600 μm abrasive), with finish polishing on a felt circle with diamond emulsion (3 μm). Metallographic studies of macro- and microstructure of unetched and etched samples and analysis of fractograms of the cast and wrought alloy were performed in optical microscope NEO-PHOT-32 (Carl Zeiss Jena, Germany), as well as in scanning electron microscope JSM-IT300LV (Jeol,

Table 3. Composition of niobium master alloy, wt.% (not more than)

| N | O | C | Fe | Si | Ta | Ti |
|------|------|------|------|------|-----|------|
| 0.05 | 0.04 | 0.06 | 0.08 | 0.03 | 0.3 | 0.07 |

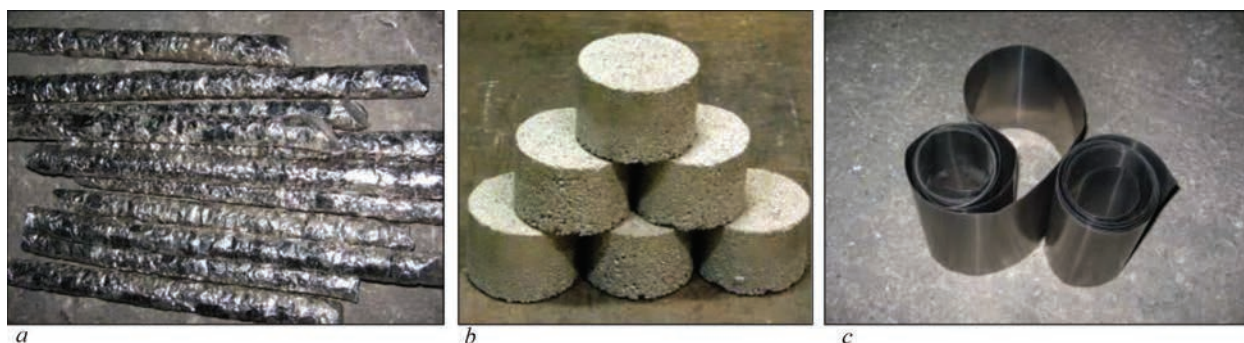


Figure 1. Charging materials: *a* — iodide zirconium TU 95.46–82, rods; *b* — sponge titanium of TG-90 grade DSTU 3079–95, briquettes; *c* — niobium NBSH-1 GOST 16100–79, sheet

Japan) with the magnification of 500–5000. To perform analysis of macro- and microstructure, the samples were etched in a solution of hydrofluoric (20 %) and nitric (20 %) acids with a glycerin base. Three samples were used for each measurement method. Investigations of the ingot material microstructure were performed using optical microscope AxioObserver 5 at magnifications of 25–200. Etching of samples for metallographic studies was performed in “Titan” reagent of $\text{HF}:\text{HNO}_3:\text{H}_2\text{O} = 1:2:6$ composition.

Characteristics of distribution of the main alloying elements in the produced powders were assessed using scanning electron microscope Olympus DSX 1000 with DSX10-SXLOB1X lens and were analyzed using LEXT Olympus Analysis program. SEM images were obtained in scanning electron microscope Hitachi SU3900 under different conditions of vacuum and accelerating voltage of 15 kV. Energy dispersive spectroscopy (EDS) was conducted using Bruker detector and Esprit software.

Mechanical parameters of the developed alloy and end rod were studied using INSTRON 8801 system, (Instron, Norwood, Massachusetts, USA). In order to determine the mechanical properties, the following parameters were assessed: tensile strength (σ_t , MPa), yield limit ($\sigma_{0.2}$, MPa), modulus of elasticity (E , GPa), relative elongation (δ , %) and reduction in area (ψ , %).

Measurements of Young’s modulus of synthesized alloys were performed by nondestructive resonance method of pulsed excitation in RFDA Professional System 24 (Belgium). Mechanical vibrations in the studied samples of a flat shape were excited by a blow from the striker. Determination of Young’s modulus was conducted by resonance frequency measurement, and the derived signal was calculated by fast Fourier transform.

TECHNICAL REQUIREMENTS TO LOW-MODULUS ALLOY OF Zr–Ti–Nb ALLOYING SYSTEM AND PRODUCTS FROM IT

Modern technology of producing commercial billets for implants is a rather complicated technical assign-

ment both as to achieving the required geometry, and as to mechanical properties of the billets.

Technological scheme of producing the billets consists of the following stages: charging, ingot melting, ingot machining, forging, rolling, drawing, heat treatment, centrifugal grinding. Producing billets from experimental Zr–Ti–Mn alloy requires development and determination of a specific scheme and modes of deformation and heat treatment:

- billet in the form of a 6 mm dia rod for the technological scheme of producing the implants;
- consumable products (50–60 mm diameter electrodes) for the technological scheme of producing powders by spraying method.

In keeping with the results of previous studies the following requirements to the billets from Zr–Nb–Ti alloy were formulated: chemical composition: Zr, at.% 51 ± 2.0 (50 wt.%); Ti, at.% 31 ± 1.5 (19 wt.%); Nb, at.% 18.0 ± 1.5 (21 wt.%); mechanical properties: ultimate strength $\sigma_t > 700$ MPa; Young’s modulus $E < 57$ GPa (considering that for the human bone E is equal to 30 GPa); requirements to billet geometry: diameter of $6 \text{ mm} \pm 2 \text{ mm}$; length of 1500–3000 mm; surface roughness $R_a 1.6\text{--}3.2$; deviation from roundness should correspond to accuracy class h7; curvature should not exceed 0.5 % of the length.

Comparison of the obtained characteristics of experimental Zr–Nb–Ti alloy by the stretching diagram shows that elasticity modulus E is in the same range for the produced alloy samples, and it is equal to 27–29 GPa. Obtained values correspond to the claimed requirements to the implant metal. The level of mechanical properties, however, is lower than that for titanium alloy, namely for rod billet from VT6 alloy. The conclusion of the technological regulations for further treatment is that deformations, as well as modes of deformation and heat treatment, should provide simultaneous shaping of the implant billet (6 mm diameter rod) with improvement of the mechanical properties at uniaxial stretching to the level of VT6 alloy.

DEVELOPMENT OF THE TECHNOLOGY OF PRODUCING Zr–Ti–Nb ALLOY, INVESTIGATION OF THE ALLOY AND PRODUCTS FROM IT

Research work by the technology of producing low-modulus Zr–Ti–Nb alloy was performed with the purpose of optimization of the technological modes of producing ingots of an alloy based on Zr–Nb–Ti system by EBM method.

The technology of cold-hearth EBM is an effective method of producing sound ingots with the possibility of using a high proportion of wastes [12].

Cold-hearth application allows not only cleaning from impurities and inclusions of different density, but also producing an ingot of a homogeneous chemical composition and sound structure. More over, cold-hearth remelting allows alloying the liquid metal during melting, as well as processing the metal melt by different reagents.

At remelting, crystallization proceeds under the conditions of continuous coming of metal into the liquid pool, heating of the liquid pool surface, and ingot cooling. These factors ensure a favourable configuration of the liquid pool and high temperature gradient at crystallization, lowering the probability of initiation and development of macrostructure defects.

The essence of EBM process (Figure 2) consists in a horizontal feed of consumable billet 4 with the set rate into the melting zone, its melting by electron beams of guns 2, 3 above cold hearth 5. As the cold hearth is filled, the liquid metal is poured into mould 6, where ingot 7 of the required length is formed.

Ingot melting was conducted in electron beam unit UE-208M into 110 mm diameter mould (Figure 3) [13].

Ingots were produced in the following sequence: calculation of the quantity of charge, allowing for metal evaporation; performing operations on initial material preparation and forming the consumable billet; preparation (cleaning of melting chamber and gun plate, cleaning the cold hearth and mould, tray cleaning, cleaning the electron gun beam guide from condensate, dust and remains of metal from previous melts) and setting up equipment (replacement of electron beam gun cathodes) and fixtures; performing melting in the specified modes; selection of samples

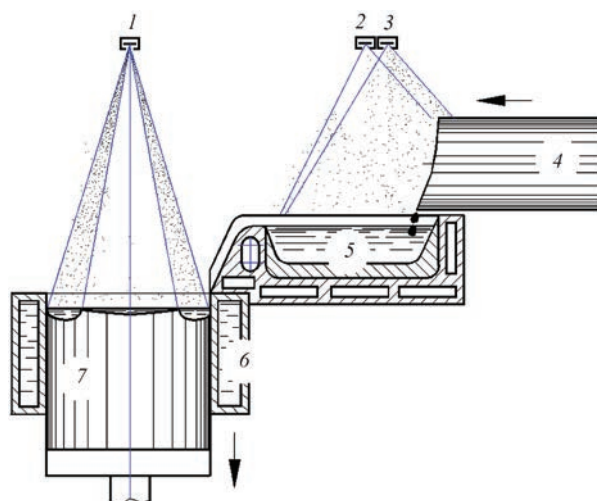


Figure 2. Scheme of cold-hearth EBM: 1–3 — electron beam guns; 4 — consumable billet; 5 — cold hearth; 6 — mould; 7 — ingot

for fast analysis of the produced ingot — chemical and gas analysis; selection of samples for mechanical testing of the produced ingot.

Calculated composition of the charge billet is given in Table 4.

During experimental melts the following technological parameters were monitored; melting rate and beam currents, accelerating voltage values. Numerical values of accelerating voltage and beam current were measured and adjusted, using instruments designed for it. Melting rate was adjusted by varying the speed of consumable billet feeding into the melting zone.

In order to determine the technological modes of conducting the EBM process to produce 60Zr–20Ti–20Nb alloy, a mathematical model was constructed of turbulent hydrodynamic and thermal processes in a cylindrical ingot of 110 mm diameter under the conditions of quasi-stationary mode of electron beam melting, which determines the dependence of the shape and depth of the metal pool in the mould on melting rate and power of electron beam heating of the melt surface.



Figure 3. Appearance of upgraded electron beam unit UE-208M

Table 4. Composition of the charge for producing ingots of 60Zr–20Ti–20Nb alloy

| Component | wt. % | kg |
|-----------|-------|------|
| Zr | 59 | 35.5 |
| Nb | 21 | 12.4 |
| Ti | 20 | 12.5 |
| Total | 100 | 60.4 |

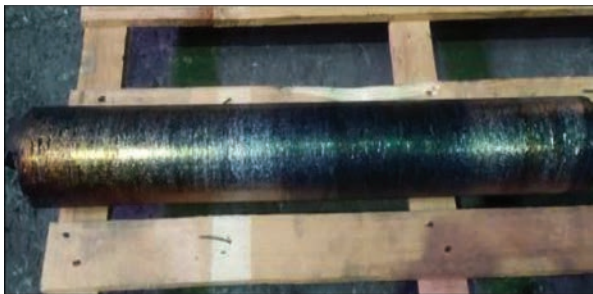


Figure 4. Ingot of 110 mm diameter of 60Zr-20Ti-20Nb alloy

It is known [9] that the flat and shallow shape of the metal pool at ingot production promotes formation of a fine homogeneous structure of the ingot metal and inhibition of the liquation processes at melt solidification. Analysis of the results of calculations by the plotted mathematical model allowed determination of the technological parameters of the stationary mode of electron beam melting which should ensure chemical homogeneity of the ingot and homogeneity of its structure, and they are the following:

**Technological parameters of electron beam melting
of a 110 mm ingot of 60Zr-20Ti-20Nb alloy**

| | |
|-------------------------------|-----|
| Total power of EB heating, kW | 110 |
| Power in the mould, kW | 20 |
| Melting rate, kg/h | 20 |

After completion of melting, the produced ingots were cooled under the conditions of vacuum in the melting chamber. EMB ingot of 110 mm diameter from experimental alloy 60Zr-20Ti-20Nb is shown in Figure 4.

The quality of the ingot external surface is satisfactory, foundry corrugations are not more than 2 mm, and no cavities, cracks or pores are revealed.

Sample selection was performed from the ingot side surface by drilling to 5 mm depth without cutting fluid application during its machining (Figure 5).

The quality of the produced ingot metal was evaluated by the results of determination of its chemical composition (Table 5). Analysis of the derived results showed that deviations of zirconium content along the ingot length from its average value do not exceed 1.7 %; titanium — 0.8 %; niobium — 0.8 % that practically completely corresponds to the requirements of technical assignment.



Figure 5. Selection of samples from 110 mm dia ingot of 60Zr-20Ti-20Nb alloy



Figure 6. Appearance of machined 110 mm dia ingot of 60Zr-20Ti-20Nb alloy

For further operations, the ingot was treated by machining (Figure 6).

The quality of the metal internal volume was studied by the method of nondestructive ultrasonic testing (UT) using UD4-76 flaw detector. No shrinkage cav-

Table 5. Chemical composition of 110 dia ingot of 60Zr-20Ti-20Nb alloy, wt. %

| Sample | Zr | Ti | Nb | O | Others |
|---------------|------|------|------|-------|--------|
| 1 | 57.5 | 19.6 | 22.4 | 0.053 | <0.6 |
| 2 | 58.7 | 18.3 | 22.4 | — | |
| 3 | 60.7 | 18.2 | 20.9 | — | |
| 4 | 58.9 | 19.7 | 20.8 | — | |
| Average value | 59.0 | 18.9 | 21.7 | 0.053 | <0.6 |



Figure 7. Appearance of 59 mm dia forgings of 60Zr–20Ti–20Nb alloy

ities, pores and other inhomogeneities were found in the ingot metal.

Work results suggest the possibility of producing by EBM sound ingots of low-modulus alloys of 60Zr–20Ti–20Nb type, designed for application as bioinert alloys for medical purposes.

DEFORMATIONAL AND HEAT TREATMENT AND SHAPING A BILLET WITH HIGHER MECHANICAL PROPERTIES

Deformational processing was performed using thermal preparation in an automatic forging complex

AKP-500 with 5 MN hydraulic press, manipulator and two heating furnaces with precise temperature control. Three-stage heating mode was performed: 700 °C for 2.5 h, then 900 °C for 1 h with subsequent transfer to the force forging at the temperature of 1000 °C for 1 h.

Forging was performed by “circle-square” scheme in the following modes: transition from 106 mm diameter to 91 mm square; transition from 91 mm square to 75 mm square; transition from 75 mm square to 60 mm square; transition from 60 mm square to

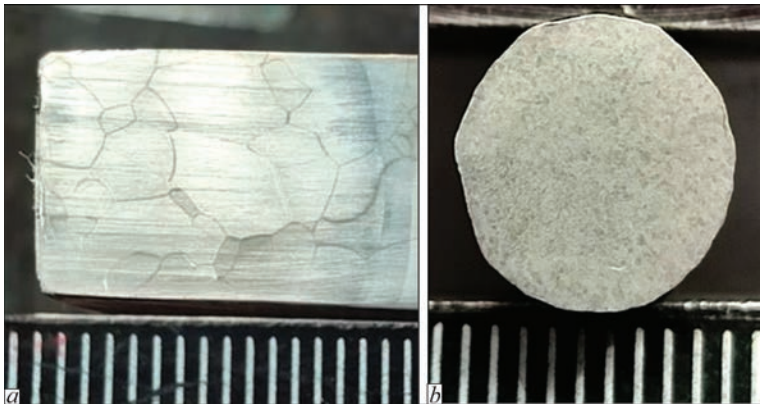


Figure 8. Macrostructure of 110 mm dia ingot after EBM (a) and of 6 mm rods from 60Zr–20Ti–20Nb alloy (b)

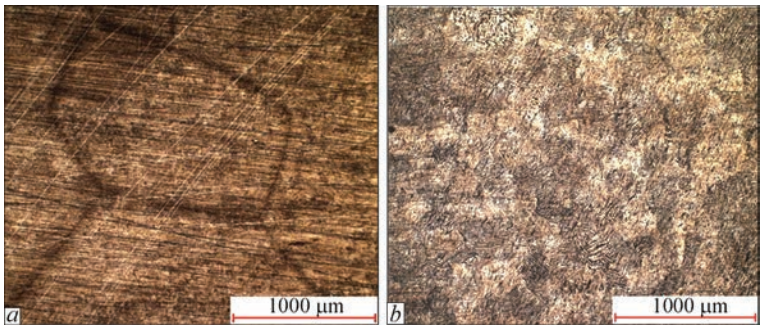


Figure 9. Microstructure of 110 mm dia ingots (a) and final 6 mm rod billets (b)

Table 6. Comparative characteristic of 6 mm dia rod billet of 60Zr–20Ti–20Nb alloy and VT6 titanium alloy for dental implants

| Alloy | Mechanical properties | | | | |
|----------------|-----------------------|----------------------|-------------------|--------------|------------|
| | σ_t , MPa | $\sigma_{0.2}$, MPa | E , GPa | δ , % | ψ , % |
| 60Zr–20Ti–20Nb | 850÷900 | 670÷700 | 28–30* 59–66** | 12 | 40–58 |
| VT6 | 830÷1254 | – | 115* 102–104** | 10 | 44 |
| Grade 5 ELI | 860 | 795 | – | 10 | 25 |

*Values of the modulus of elasticity were determined by calculations from stretching diagram of samples for mechanical testing.
**Values of the modulus of elasticity were determined by the method of pulsed excitation in RFDA Professional System 24.

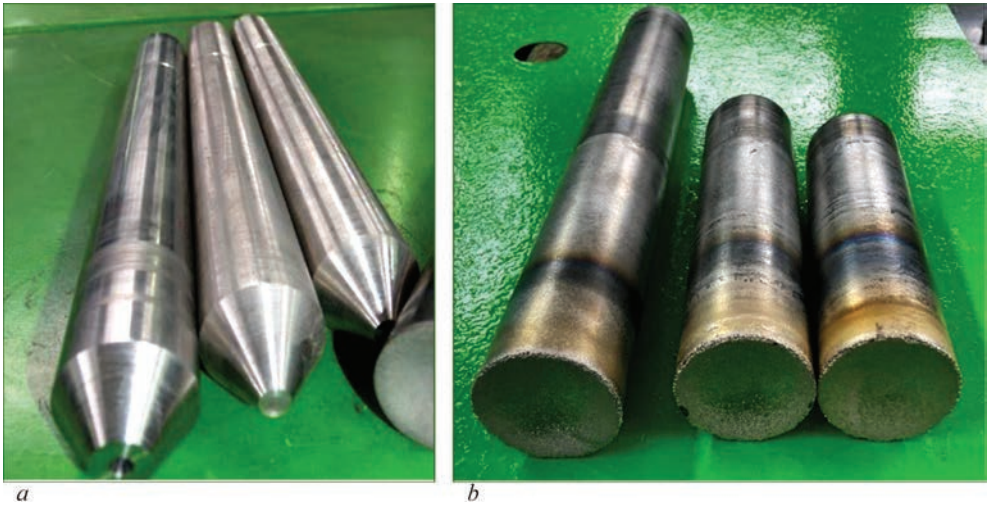


Figure 10. Electrodes of 50 mm dia from 60Zr–20Ti–20Nb alloy to produce spherical powders before spraying (*a*) and after spraying (*b*)

59 mm diameter; metal heating in the forging furnace after each pass, and cooling of the forging in air.

Produced forgings are shown in Figure 7.

Rod forging was followed by rolling and drawing to 6 mm diameter. As a result, the rod billets have the fol-

lowing geometrical characteristics: 6 mm diameter; up to 3150 mm length; h7 class of accuracy; surface roughness of Ra0.8. Macrostructure of 6 mm diameter rods of 60Zr–20Ti–20Nb alloy is shown in Figure 8.

Macrostructure analysis showed that β -primary grains of the ingots of equiaxed type with a coarse fringe of up to 5 μm size (Figure 8, *a*) were refined to fine-grained macrostructure in the rods (Figure 8, *b*).

Results of studying the microstructure revealed that the microstructure was refined to 50–60 μm size (Figure 9).

Microstructural analysis showed that it changes from cast coarse-grained structure of 150–200 μm primary grains to deformed fine equiaxed structure with platelike submicrostructure.

Mechanical properties of the produced rod of 6 mm diameter of 60Zr–20Ti–20Nb alloy in comparison with titanium alloy VT6/Grade 5 are given in Table 6.

One can see from the comparative data that the rod billet from an alloy based on Zr–Ti–Nb system has minimal value of the modulus of elasticity (27.6 GPa), which is 3 times lower than that of VT6 alloy (115 GPa) and it is close to the value of modulus of elasticity of the human bone (30 GPa). It gives grounds to talk about improvement of biocompatibil-

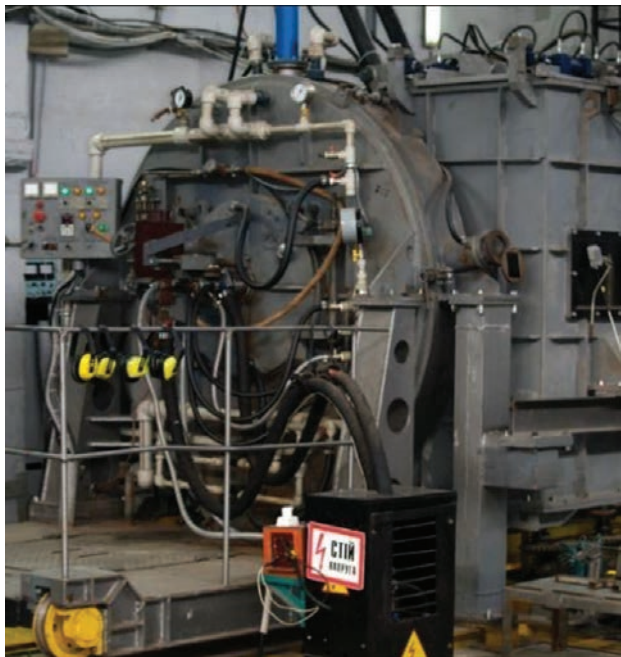


Figure 11. UTsR-4 unit for centrifugal spraying

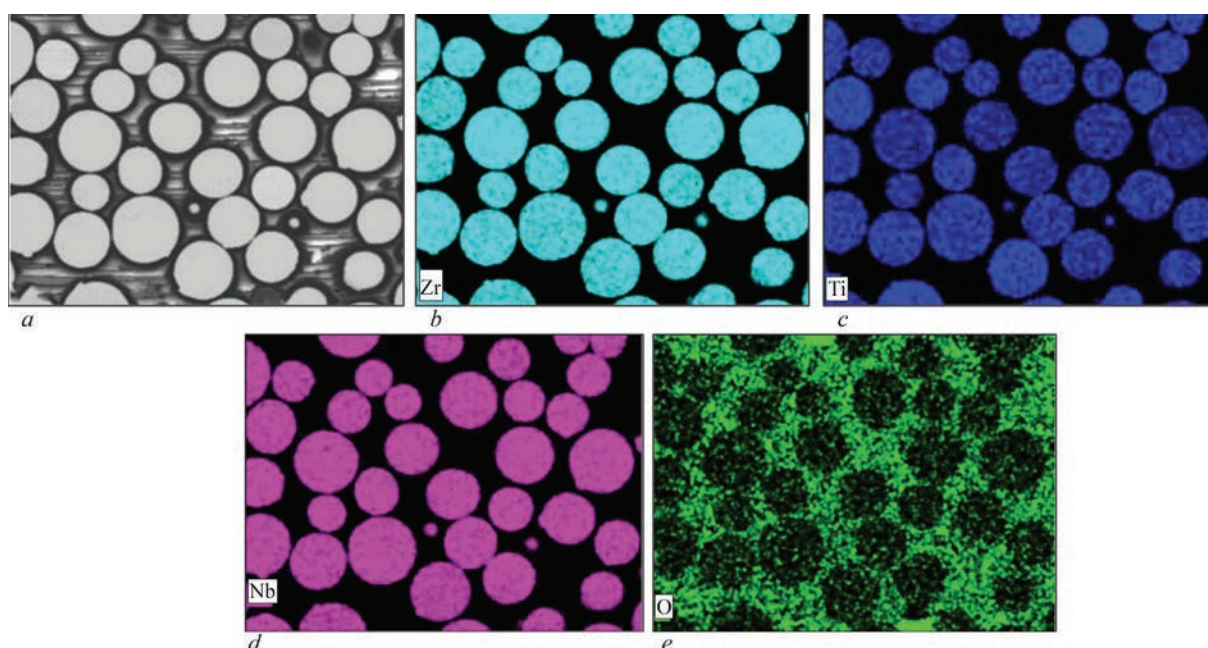


Figure 12. Electronic photo of 60Zr–20Ti–20Nb powder (*a*) and maps of distribution of zirconium (*a*), titanium (*b*), niobium (*c*) and oxygen (*e*) over analysis zone

Table 7. Fractional composition of produced metal powders from Zr–Ti–Nb alloy

| Fraction | Bulk density, g/cm ³ | Weight, g |
|----------|---------------------------------|-----------|
| +200 | 4.2 | 900 |
| +180 | 4.19 | 128 |
| –140+125 | 4.00 | 2654 |
| –90+56 | 3.97 | 1589 |
| –56+40 | – | 95 |
| –40 tray | 3.96 | 261 |

ity. At the same time, load resistance corresponds to that of analogous VT6 alloy that confirms the level of mechanical properties of the zirconium alloys.

PRODUCING POWDERS OF Zr–Ti–Nb ALLOY

Forgings of 59 mm diameter from 60Zr–20Ti–20Nb alloy were used to produce by machining a test batch of electrodes of 50 mm diameter for manufacturing spherical powders by the method of centrifugal plasma spraying [14] (Figure 10).

Appearance of UTsR-4 unit for centrifugal spraying is shown in Figure 11.

Produced metal powders of 60Zr–20Ti–20Nb alloy were sifted on vibration sieves into different fractions.

An example of fractional composition of the produced metal powders of Zr–Ti–Nb alloy is given in Table 7.

The main criterion of powder quality is the chemical composition of the powders, alongside the shape and fractional composition. Analysis of investigation results led to the conclusion that the microstructure (Figure 12, *a*) is homogeneous, without inclusions,

pores or structure inhomogeneities. Results of analysis of chemical composition of the main elements and oxygen impurities showed that they are uniformly distributed (Figure 12, *b–e*). No concentrational heterogeneities of the elements were found.

Thus, the scientific and engineering solutions on melting ingots of 60Zr–20Ti–20Nb alloy allowed producing rods and spherical powders, meeting all the technological and service requirements of TU U24.4-43658421-002:2021 “Powder from an alloy based on zirconium–titanium–niobium system”.

CONCLUSIONS

1. Given results of research work indicate the possibility of producing by EBM the ingots of low-modulus alloys based on zirconium of 60Zr–20Ti–20Nb type designed for application as bioinert alloys for medical purposes.

2. A technology was developed to produce Zr–Ti–Nb alloy by electron beam melting, with satisfactory distribution of alloying components and homogeneous defectfree structure.

3. A scheme of deformational processing of the billet is proposed which allowed producing the required geometry of a rod of 6 mm diameter, 3150 mm length, with deviation from roundness in keeping with h7 accuracy class and surface roughness of Ra 0.8. As a result of conducting testing on samples from a rod billet, evaluation of mechanical properties of experimental 60Zr–20Ti–20Nb alloy was obtained: ultimate strength of 850–900 MPa, elongation of 12 %.

4. Obtained evaluations showed that the rod billet from experimental β -Zr alloy of 60Zr–20Ti–20Nb

composition has the modulus of elasticity $E = 28\text{--}30$ GPa (calculated from stretching diagrams of samples for mechanical testing) and modulus of elasticity $E = 59\text{--}66$ GPa (determined by the method of pulsed excitation in RFDA Professional System 24) that is much lower than in VT6 alloy ($E = 102\text{--}115$ GPa) and is closer to the value of modulus of elasticity of the human bone ($E = 30$ GPa).

5. Presented results are indicative of practical possibilities of producing consumable materials for implants (6 mm diameter rods) and spherical powders for additive technologies of manufacturing high-precision implants, where the microstructure is uniform without inclusions, pores or structural inhomogeneities, corresponding to all technological and service requirements. Results of the conducted studies were used to prepare technical conditions TU U24.4-43658421-002:2021 “Powders from an alloy of zirconium–titanium–niobium” system.

REFERENCES

1. Liu, Xuanyong, Chu, Paul K., Ding, Chuanxian (2004) Surface modification of titanium, titanium alloys, and related materials for biomedical application. *Materials Sci. and Eng.: R: Reports*, 47(3), 49–121. DOI: <https://doi.org/10.1016/j.mser.2004.11.001>
2. Elias, C.N., Lima, J.H.C., Valiev, R., Meyers, M.A. (2008) Biomedical applications of titanium and its alloys. *JOM*, 60(3), 46–49. DOI: <https://doi.org/10.1007/s11837-008-0031-1>. S2CID 12056136
3. Niinomi, M. (2000) Development of high biocompatible titanium alloys. *Func. Mater.*, 20, 36–44.
4. Fellah, Mamoun, Labaiz, Mohamed, Assala, Omar et al. (2014) Tribological behavior of Ti–6Al–4V and Ti–6Al–7Nb alloys for total hip prosthesis. *Advances in Tribology*, 451387. DOI: <https://doi.org/10.1155/2014/451387>
5. Lopez, M.F., Gutierrez, A., Jimenez, J.A. (2002) In vitro corrosion behaviour of titanium alloys without vanadium. *Electrochimica Acta*, 47(9), 1359–1364. DOI: [https://doi.org/10.1016/S0013-4686\(01\)00860-X](https://doi.org/10.1016/S0013-4686(01)00860-X)
6. Ivasyshyn, O.M., Skyba, I.O., Karasevska, O.P., Markovskiy, P.E. (2013) *Biocompatible alloy with low modulus of elasticity based on zirconium–titanium system (variants)*. Ukraine, Pat. 102455 [in Ukrainian].
7. Niinomi, M. (2008) Mechanical biocompatibilities of titanium for biomedical applications. *J. of the Mechanical Behavior of Biomedical Materials*, 1, 30–42. DOI: <https://doi.org/10.1016/j.mbbm.2007.07.001>
8. Mishchenko, O., Ovchynnykov, O., Kapustian, O., Pogorielov, M. (2020) New Zr–Ti–Nb alloy for medical application: Development, chemical and mechanical properties, and biocompatibility. *Materials*, 13(6), 1306. DOI: <https://doi.org/10.3390/ma13061306>
9. Berezos, V.O., Akhonin, D.S. (2023) Electron beam melting of titanium alloys for medical purposes. *Suchasna Elektrometal.* 2, 5–13 [in Ukrainian]. DOI: <https://doi.org/10.37434/sem2023.02.01>
10. Ladokhin, S.V., Levitsky, M.I., Chernyavsky, V.B. et al. (2007) *Electron beam melting in foundry*. Kyiv, Stal [in Russian].
11. Grechanyuk, N.I., Kulak, L.D., Kuzmenko, N.N. et al. (2017) Melting of ingots of Ti–Nb–Si–Zr system titanium alloys by the method of electron beam melting. *Suchasna Elektrometal.*, 2, 17–20 [in Russian]. DOI: <https://doi.org/10.15407/sem2017.02.03>
12. Akhonin, S., Pikulin, O., Berezos, V. et al. (2022) Determining the structure and properties of heat-resistant titanium alloys VT3-1 and VT9 obtained by electron-beam melting. *Eastern-European J. of Enterprise Technologies*, 5(12)(119), 6–12. DOI: <https://doi.org/10.15587/1729-4061.2022.265014>
13. Akhonin, S.V., Pikulin, A.N., Berezos, V.A. et al. (2019) Laboratory electron beam unit UE-208M. *Suchasna Elektrometal.*, 3, 15–22 [in Russian]. DOI: <http://dx.doi.org/10.15407/sem2019.03.03>
14. Ovchynnykov, O.V., Khaznaferov, M.V. (2022) *Introduction to additive technologies of nonferrous metals*. Kyiv, Naukova Dumka [in Ukrainian].
15. <https://powdermet.com.ua/>

ORCID

O.V. Ovchynnykov: 0000-0002-5649-1094,
V.O. Berezos: 0000-0002-5026-7366,
V.S. Yefanov: 0000-0002-6363-4081,
D.S. Akhonin: 0009-0000-2054-4054,
D.I. Mozulenko: 0000-0002-0428-9265

CONFLICT OF INTEREST

The Authors declare no conflict of interest

CORRESPONDING AUTHOR

V.O. Berezos

E.O. Paton Electric Welding Institute of the NASU
11 Kazymyr Malevych Str., 03150, Kyiv, Ukraine.
E-mail: titan.paton@gmail.com

SUGGESTED CITATION

O.V. Ovchynnykov, V.O. Berezos, V.S. Yefanov, D.S. Akhonin, D.I. Mozulenko (2024) Development of the technology of producing a biocompatible alloy based on zirconium–titanium–niobium system for medical implants. *The Paton Welding J.*, 11, 36–44. DOI: <https://doi.org/10.37434/tpwj2024.11.05>

JOURNAL HOME PAGE

<https://patonpublishinghouse.com/eng/journals/tpwj>

Received: 16.05.2024

Received in revised form: 02.07.2024

Accepted: 02.09.2024

**XXIII INTERNATIONAL
INDUSTRIAL FORUM - 2025**
Kyiv, May 27–29, www.iec-expo.com.ua